ELSEVIER

Journal of Nuclear Materials 255 (1998) 250–262

journal of nuclear materials

Modelling of hydrogen absorption by zirconium alloys during high temperature oxidation in steam

M.S. Veshchunov *, A.V. Berdyshev

Nuclear Safety Institute (IBRAE), Russian Academy of Sciences, B. Tul'skaya, 52, Moscow, 113191, Russian Federation

Received 11 August 1997; revised 23 January 1998

Abstract

A model is developed for description of hydrogen absorption by Zr alloys during high temperature oxidation in steam, based on the detailed experimental results of recent tests on the kinetics of hydrogen absorption by Zr–1Nb cladding during steam oxidation in the temperature range from 900 to 1200°C. The standard consideration of the steam oxidation process in the framework of the coupled anodic/cathodic reactions at the two oxide interfaces (gas/oxide and oxide/metal) is modified, taking into account that hydrogen may intrude into oxide in the form of positively charged protons. For quantitative description of hydrogen behaviour by this mechanism, mass transfer in the three layers, gas, oxide and metal, and at corresponding interfaces, gas/oxide and oxide/metal, is self-consistently considered. Numerical solution of the model generally confirms the main conclusions of simplified analytical treatment and furnishes a satisfactory fitting between measured kinetic curves and calculations.

1. Introduction

Hydrogen absorption by zirconium alloys during their oxidation in steam was studied in the last three decades since the primary concern of this process is the embrittlement which might occur during pressurised water reactors normal operation (see, for example, review Ref. [1]). It was shown that, in parallel with the oxide film formation process in water or steam, a fraction of hydrogen generated by the decomposition of water entered the metal. The relationship between the amount of oxidation occurring and the amount of hydrogen absorbed is not a simple function, although it follows a characteristic pattern which seems to be general for all zirconium alloys, provided the analytical technique is sensitive enough to distinguish changes in the 'uptake fraction' (that fraction of hydrogen liberated by the corrosion process during any time period and which is absorbed by the metal).

Far fewer experimental data are available for the high temperature hydriding. In the literature one can frequently find only observations or trends instead of quantitative relations. Recently, new tests [2–6] were performed in which the absorption phenomena were studied at high temperatures corresponding to the conditions of a severe accident at nuclear power plants. In Ref. [2], data on hydrogen uptake by Zr–1Nb during oxidation were given in the temperature range 900–1100°C. The concentration of absorbed hydrogen was in the range 100–1000 ppm after steam exposure for 10–30 min. It corresponds to a relative hydrogen uptake of 10–70%. Under the same experimental conditions far lower hydrogen concentration in Zircaloy-4 was found (4–100 ppm, corresponding to a relative hydrogen uptake of 1–10%).

In the latest tests [6] hydrogen uptake was also studied simultaneously with measurements of Zr–1Nb alloy oxidation kinetics in steam under 1 bar pressure in the temperature interval 900–1200°C. Clear qualitative tendencies and quantitative correlations between oxidation kinetic rates and hydrogen uptake have been revealed in these experiments. Below 1050°C the hydrogen content of oxidised samples increased constantly with time up to the longest

* Corresponding author. Fax: +7-095 958 0040, 952 3701; e-mail: vms@ibrae.ac.ru.

0022-3115/98/$19.00
PII: S0022-3115(98)00018-X

exposition (10^4 s) being proportional to the oxidation mass gain. At higher temperatures (1100–1200°C) a maximum was reached after a relatively short time (500–1000 s), this content being definitely less at the same mass gains compared with those at lower temperatures.

On the basis of the detailed experimental studies [6], the development of a theoretical model of the hydrogen absorption phenomena is attempted in the present paper.

2. Hydrogen penetration mechanism through the oxide layer

In order to develop a model for hydrogen absorption by the Zr cladding in the course of its oxidation in steam, firstly it is necessary to reveal a physical mechanism of hydrogen migration through the ZrO_2 scale. In surveying the results on hydrogen absorption one should distinguish between two possible routes; first, direct reaction with molecular hydrogen (gaseous hydriding), and second, absorption of hydrogen liberated by the decomposition of water or steam during the oxidation process and absorbed as part of the oxidation mechanism [1].

As it became clear from studies of gaseous hydriding of ZrO_2 slabs, both the solubility and the diffusivity of the solute in the solid are extremely small. For example, in the tests [7] the solubility and release kinetics of hydrogen in single-crystal zirconia were investigated by the infusion–extraction method. Equilibration in hydrogen at pressures between 1.4 and 11 bar and at temperatures from 1300 to 1600°C produced H/Zr ratios varying from 4×10^{-5} to 1.3×10^{-4}. The solubility behaviour and the kinetics of release indicated that hydrogen atoms are strongly trapped by distinct binding sites in the solid with detrapping activation energies from 67 to 80 kJ/mol.

Such small values of the solubility and mobility apparently cannot provide rather large quantities of hydrogen transported through the oxide and dissolved in the metal phase as observed in the above mentioned tests [2–6] on absorption of hydrogen during the oxidation process. Indeed, in these tests a fraction of hydrogen generated by decomposition of the steam entered the metal in the course of high-temperature zirconium alloy (Zr-4 or Zr–1Nb) oxidation reached several tens percents. An analogous behaviour has been also observed at lower temperatures (characteristic to reactor normal operation conditions) [1]. In particular, in a recent paper [8] oxidation and hydrogen uptake of Zr based Nb alloys were studied as functions of Nb content and heat treatment at 400°C under 100 bar steam atmosphere. The percentage of hydrogen uptake in these tests after 58 days oxidation varied from 10 to 40% depending on the Nb content.

An important conclusion drawn by Park and Olander [7] was that in the result of H_2 gas interactions with zirconia (gaseous hydriding) hydrogen apparently penetrates into the solid phase in the form of a neutral atom. Assignment of dissolved hydrogen as a neutral atom rather than as a proton was necessary to produce the dependence of solubility on the square root of the pressure (i.e., Sieverts' law) observed in Ref. [7].

On the other hand, in tests Wagner [9] measured the solubility of water vapour in yttria-stabilized zirconia. The dissolution process was interpreted in terms of the reaction:

$$H_2O(g) + V_o^{2+} = 2H_i^+ + O_o(ox), \quad (1)$$

where $O_o(ox)$ is an oxygen ion on a regular lattice site, V_o^{2+} is a doubly charged anion vacancy, H_i^+ is an interstitial proton. This reaction predicts the variation of the solubility S with the square root of the water vapour pressure, $S \propto p_{H_2O}{}^{1/2}$, which was observed in the experiment.

The dissolution process observed in Ref. [9] differs in the charge state of the hydrogen in the gas from that in Ref. [7]; with H_2, the hydrogen is neutral, whereas, with H_2O, the hydrogen has a single positive charge. It appears that hydrogen in the solid oxide retains the charge state that it had in the gas, so that the two dissolution processes are fundamentally different [7].

It is important also to notice that amounts of dissolved hydrogen in the two tests [7,9] were quite comparable ($H/Zr \simeq 10^{-5}$) despite $\simeq 8$ orders of magnitude difference of the partial H_2 pressures in the gas phases. In the test given in Ref. [7], $p_{H_2} \approx 1$–10 bar at $T = 1300$–1600°C, whereas in Ref. [9] (performed in the steam atmosphere under the pressure $p_{H_2} \approx 10^{-2}$ bar at temperatures 900–1000°C) the partial pressure of H_2 can be evaluated as $p_{H_2} \approx 10^{-7}$ bar. Such a significant difference of the hydrogen solubility in the two tests apparently confirms the conclusion about fundamentally different dissolution mechanisms occurred under conditions of these tests.

In addition to the measurement of solubility, Wagner also measured the kinetics of water uptake by yttria-stabilized zirconia [9]. The data were interpreted in terms of diffusion of interstitial hydrogen in the solid. The measured diffusivities were rather high (8×10^{-7} cm^2 s^{-1} at 890°C and 1.3×10^{-6} cm^2 s^{-1} at 990°C). This discrepancy with the results of the tests [7] (in which an extremely low mobility of hydrogen owing to strong trapping was detected) was also attributed in Ref. [7] to the nature of the diffusing species in Wagner's experiments (protons rather than neutral hydrogen atoms). A possible explanation of a very high mobility of protons in comparison with neutral hydrogen atoms is that both protons and oxygen ions must penetrate the solid at the same rate to preserve local electrical neutrality in the crystal. Since the diffusivity of negatively charged oxygen ions in zirconia is rather high, they carry along positively charged protons in the same direction.

As mentioned earlier, it is easy to estimate that the extremely small solubilities and diffusivities of the neutral hydrogen atoms in the zirconia measured in Ref. [7] cannot provide significant hydrogen transport through the oxide layer into the metal observed in the tests [2–6] on the zirconium alloys oxidation in steam. Therefore, these observations can be naturally explained only by the suggestion that the hydrogen dissolution in the oxide during Zr oxidation in steam takes place by the alternative mechanism, i.e., in the form of positively charged protons rather than neutral atoms.

In accordance with this conclusion, a standard consideration of the Zr oxidation mechanism in steam should be modified and completed. It is usually proposed that hydrogen absorption proceeds in three steps (see, for example Ref. [1]). First, reaction of an adsorbed water molecule H_2O with an anion vacancy V_o^{2+} to leave two protons $2H_{ad}^{+}$ on the surface and an oxygen anion $O_o(ox)$:

$$H_2O(g) + V_o^{2+} = 2H_{ad}^{+}(ox) + O_o(ox). \quad (2)$$

Second, discharge of the protons on the surface by electrons migrating from the oxide/metal interface, i.e., cathodic reaction at the oxide/gas interface:

$$H_{ad}^{+}(ox) + e_{\beta}(ox/g) = H_{ad}(ox), \quad (3)$$

and anodic reaction at the metal/oxide interface:

$$ZrO_2(ox) + 2V_o^{2+} + 4e_{\alpha}(m/ox) = Zr(m) + 2O_o(ox). \quad (4)$$

Hydrogen adsorbed on the ZrO_2 surface may be either released as hydrogen gas molecules:

$$2H_{ad}(ox) = H_2(g), \quad (5a)$$

or absorbed in the oxide phase:

$$H_{ad}(ox) = H_{ab}(ox), \quad (5b)$$

Absorbed hydrogen $H_{ab}(ox)$ should then diffuse through the matrix oxide (see also Ref. [8]).

However, in accordance with the above presented consideration and estimations, an amount of hydrogen absorbed via Eq. (5b) is extremely small and cannot provide the observed (in the steam oxidation tests) mass transfer to the metal phase. For this reason, it should be proposed that only a part of adsorbed protons H_{ad}^{+} is discharged at the oxide/gas interface by electrons in accordance with Eq. (3). The remaining part penetrates into the oxide in the form of protons:

$$H_{ad}^{+}(ox) = H_{ab}^{+}(ox), \quad (6)$$

diffuses through the oxide and discharges by electrons only at the oxide/metal interface:

$$H_{ab}^{+}(ox) + e_{\alpha}(ox/m) = H_{ab}(m). \quad (7)$$

As a result, the behaviour of the absorbed hydrogen at the gas/oxide interface is described by the same chemical Eq. (1) (obtained by superposition of Eqs. (2) and (6)), as in the tests [9] on the water vapour dissolution:

$$H_2O(g) + V_o^{2+} = 2H_{ab}^{+} + O_o(ox),$$

and, thus, obeys the same quantitative dependencies, i.e., high solubilities and diffusivities in the oxide.

Finally, the system of equations describing chemical processes on the oxide surface should be completed by the equation specifying possible transition of the oxygen anions $O_o(ox)$ to the gas molecules $O_2(g)$:

$$2O_o(ox) = O_2(g) + 2V_o^{2+} + 4e_{\beta}(ox/g), \quad (8)$$

being there in equilibrium with dissociating water molecules:

$$2H_2O(g) = O_2(g) + 2H_2(g). \quad (9)$$

3. Modelling of hydrogen uptake

For quantitative description of hydrogen uptake by Zr during its oxidation in steam, the mass transfer in the three layers, gas, oxide and metal, and at corresponding interfaces, gas/oxide and oxide/metal, should be considered.

3.1. Mass transfer in the gas phase

Gas phase mass transfer is estimated using the analogy between heat and mass transfer. Under conditions of the laboratory tests [6] ($p_{H_2O} \approx 1$ bar, $T_{steam} \approx 450$°C, steam supply rate 7.5 mg/s, corresponding to steaming velocities ≈ 10 cm/s and the Reynolds number, Re ≈ 10) the laminar regime of the steam flow occurs. In this regime, the mass transfer coefficient k_i of the i-th species in the gas phase is estimated as

$$k_i \approx 3.7 D_i/d, \quad (10)$$

where D_i is the effective diffusivity of the gas species, d is the hydraulic diameter of the flow channel.

However, it should be taken into account that the above presented value of the mass transfer coefficient is valid only for long enough cladding tubes, namely with lengths more than $h \approx (0.1–1)\mathrm{Re}(d/2)$ [10]. In the tests [6], $d \approx 10$ mm and thus the value of the transition region h is quite comparable with the whole length of short cladding segments 40 mm. In this case the mass transfer coefficient becomes dependent on the axial position x of the tube slowly decreasing to the asymptotic value expressed by Eq. (10), obeying an axial dependence $x^{-1/2}$ ([10]). For more definite results it is recommended to reproduce such tests with longer cladding tubes (> 40 cm). Moreover, the factor 3.7 in Eq. (10) was obtained in Ref. [10] for a more simple tube flow geometry and generally should be recal-

culated for an annular flow geometry with mass transfer flux directed to the inner (i.e., sample) surface. For these reasons, the value of the effective mass transfer coefficient in Eq. (10) may be considered only as an approximate and qualitative one.

In the simplified consideration of the oxidation process it is usually proposed that the gas phase transport equation describes equimolar counterdiffusion, since one mole of water decomposed at the surface produces one mole of H_2 that returns to the bulk gas (compare, for example, with Ref. [11]). Thus, such an approach involuntary provides conservation of a constant pressure in the bulk of the gas phase.

However, under real conditions of considerable hydrogen absorption additional convection (Stefan) flows in the gas should be taken into account. Therefore, mass fluxes of the three gas components (steam, hydrogen and oxygen) take the form

$$J_i^{(g)} = k_i\big(c_i(s) - c_i(b)\big) - c_i(s)\,\nu, \tag{11}$$

where $i = 1,2,3$ denote H_2, O_2, H_2O, respectively, $c_i = p_i/RT$ is the molar density of the i-th component in the gas mixture with corresponding partial pressure p_i, indices s and b designate values near the oxide surface and in the bulk of the gas phase (outside the diffusion boundary layer), respectively (see Fig. 1), ν is the velocity of the convection flows which afford constant total pressure in the gas, $p_{tot} = p_{H_2O} + p_{H_2} + p_{O_2} = 1$ bar.

Conservation laws for the three components at the oxide surface take the form

$$k_1\big(c_1(s) - c_1(b)\big) - c_1(s)\,\nu = J_{diss} - (1/2)\,J_H^{(ox)}, \tag{12}$$

$$k_2\big(c_2(s) - c_2(b)\big) - c_2(s)\,\nu = (1/2)\,J_{diss} - (1/2)\,J_0^{(ox)}, \tag{13}$$

$$k_3\big(c_3(s) - c_3(b)\big) - c_3(s)\,\nu = -J_{diss}, \tag{14}$$

where J_{diss} specifies the dissociation flux of the H_2O molecules at the oxide surface (see Fig. 1), $J_H^{(ox)}$, $J_O^{(ox)}$ are the diffusion fluxes of the two components (protons and oxygen anions) in the oxide phase.

Since only two among the three variables c_i are independent ($c_1 + c_2 + c_3 = p_{tot}/RT$) the multi-component Stefan–Maxwell equations for their interdiffusion fluxes result in a simple relationship:

$$k_3\big(c_3(s) - c_3(b)\big) = -\big[k_1\big(c_1(s) - c_1(b)\big) + k_2\big(c_2(s) - c_2(b)\big)\big]. \tag{15}$$

In the considered case of small concentrations of the two gas components O_2 and H_2 (which are the products of equilibrium dissociation of H_2O in the gas), the effective diffusivities (see Eq. (10)) of these molecules are very close to the binary diffusivities in the H_2O/H_2 and H_2O/O_2 mixtures and thus the mass transfer coefficients k_1 and k_2 are well defined values.

It should be noted that the three Eqs. (12)–(14) are written in the form analogous to the case when dissociation of H_2O molecules in the bulk of the gas phase is not considered and the two components H_2 and O_2 are independent. In the real situation a consideration of mutual transformations of the components significantly modifies the interdiffusion fluxes in the bulk of the gas phase. The local gas composition is determined by the equilibrium reaction $2H_2O(g) = O_2(g) + 2H_2(g)$ and for this reason obeys the mass action law:

$$\ln p_{O_2} + 2\ln p_{H_2} = 2\ln p_{H_2O} + 2\Delta G/RT, \tag{16}$$

where in accordance with [10]

$$\Delta G/RT = 6.61 - 29{,}600/T. \tag{16'}$$

This equation provides an additional restriction to the solution of the diffusion problem in the gas phase for the two components H_2 and O_2 which at present cannot be considered as independent.

Nevertheless, as demonstrated in Appendix A, despite this limitation the hydrogen flux at the gas/oxide interface completely retains its form, Eq. (A.13), whereas the oxygen flux—only partially, since a finite renormalisation of the mass transfer coefficient $k_2 \to k_2'$ (in accordance with Eq. (A.14)) is necessary in Eq. (13).

Superposition of Eqs. (12)–(15) results in a simple relationship for the convection velocity in the gas:

$$(c_1 + c_2 + c_3)\,\nu = (1/2)\big[J_O^{(ox)} + J_H^{(ox)} - J_{diss}\big]. \tag{17}$$

Simple estimations show that in the initial stage of the oxidation process the surface hydrogen pressure $p_{H_2}(s)$ exceeds the corresponding bulk value $p_{H_2}(b)$ by several orders of magnitude, continuously reduces with time and finally reaches the bulk value in the end of the process. This means that during the most part of the oxidation time an inequality $p_{H_2}(s) \gg p_{H_2}(b)$ is valid. In accordance with Eq. (16), this leads to $p_{O_2}(s) \ll p_{O_2}(b)$ and, therefore,

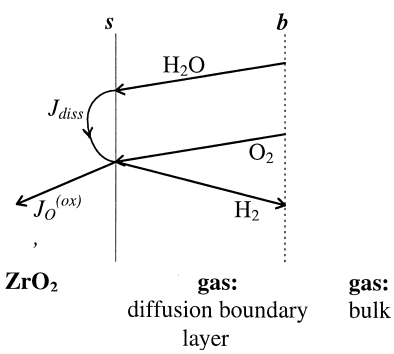

Fig. 1. Schematic representation of flux balances at the gas/oxide interface.

$\Delta p_{O_2} \ll \Delta p_{H_2}$ (since $p_{H_2}(b) \approx 2p_{O_2}(b)$). Owing to these inequalities, the convection term gives input only in the steam flux $J^{(g)}_{H_2O}$ in Eq. (14). For the same reason, oxygen flux in the gas phase $J^{(g)}_{O_2}$ can be generally neglected in Eqs. (12)–(15); in particular, Eq. (13) can be simplified:

$$J^{(ox)}_O \approx J_{diss}, \tag{18}$$

as well as Eq. (14) after substitution of Eqs. (15) and (17):

$$k_1 c_1(s) + (1/2) J^{(ox)}_H = J^{(ox)}_O, \tag{19}$$

After substitution of Eq. (18) into Eq. (19) one finally gets a relationship

$$k_1 c_1(s) + (1/2) J^{(ox)}_H = J^{(ox)}_O, \tag{20}$$

which has a clear physical sense: neglecting the small flux $J^{(g)}_{O_2}$, the flux $J^{(ox)}_O$ is exactly equal to the steam flux $J^{(g)}_{H_2O}$ which delivers oxygen to the oxide surface through the gas; in its turn, of hydrogen the solid phase flux $J^{(ox)}_H$ matches the resulting flux delivering hydrogen (via H_2 and H_2O molecules) to the surface through the gas $2(k_1 c_1(s) - J^{(g)}_{H_2O}) = 2(k_1 c_1(s) - J^{(ox)}_O)$.

3.2. Mass transfer through the oxide / gas interface

The derived Eq. (20) determines a relation between the fluxes of various components in the gas and solid phases. In order to calculate these fluxes, it is necessary to determine relations between concentrations of these components at the oxide/gas interface.

Results of numerous investigations of the high-temperature Zr cladding oxidation kinetics evidence that the rate determining step of this process (under unlimited steam supply conditions) is the oxygen diffusion in the oxide phase. In particular, a parabolic time law of the oxidation kinetics observed in such tests (as well as in Ref. [6]) directly confirms this statement. This means that surface kinetic processes of oxygen transition from the gas to the oxide phase are so quick (in comparison with the bulk diffusion processes), that the condition of thermodynamic equilibrium for the oxygen component prevails at the gas/oxide interface.

For these reasons, it can be concluded that at least a part of the chemical reactions at the gas/oxide interface considered in Section 2 should be regarded as equilibrium:

- dissolution of water molecules at the oxide surface, Eq. (1) (obtained by superposition of Eqs. (2) and (6)):

$$H_2O(g) + V^{2+}_o = 2H^+_{ab} + O_o(ox);$$

- oxygen transition from the oxide to the gas phase, Eq. (8):

$$2O_o(ox) = O_2(g) + 2V^{2+}_o + 4e_\beta(ox/g);$$

- dissociation of water molecules in the gas phase, Eq. (9):

$$2H_2O(g) = O_2(g) + 2H_2(g).$$

Correspondingly, for each of these equilibrium reactions the mass action law can be applied:

$$p_{H_2O}(s) C_\nu = \alpha C^2_{H+}, \tag{21}$$

$$p_{H_2O}(s)^2 = k p_{H_2}(s)^2 p_{O_2}(s), \tag{22}$$

$$p_{O_2}(s) C^2_\nu C^4_e = \beta, \tag{23}$$

where $p_i(s)$ is the i-th component partial gas pressure at the interface, α, β, k are the equilibrium constants of the corresponding chemical reactions (the constant k is determined in Eqs. (16) and (A.3)), C_ν, C_e, C_{H+} are concentrations of anion vacancies V^{2+}_o, electrons and protons in the oxide near the interface, respectively.

An additional assumption about thermodynamic equilibrium at the interface for the hydrogen component, which obeys a superposition of the chemical Eqs. (3) and (5a):

$$H^+_{ab}(ox) + e_\beta(ox/g) = (1/2)H_2(g),$$

leading to the corresponding mass action law:

$$C^2_{H+} = \gamma p_{H_2}(s) / C^2_e, \tag{24}$$

is not really important for further calculations, since it results only in an additional relationship among the equilibrium constants of Eqs. (21)–(24):

$$\alpha\gamma / k\beta^{1/2} = 1.$$

Mass transfer of various components at the gas/oxide interface determined by the above described chemical processes can be schematically represented by a diagram in Fig. 2.

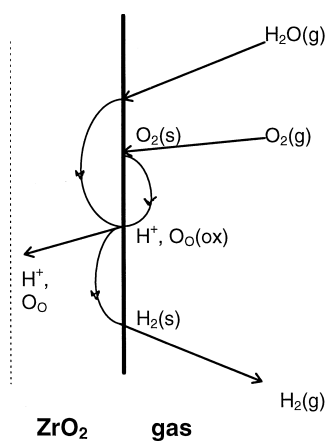

Fig. 2. Schematic representation of chemical reactions at the gas/oxide interface.

The charge neutrality condition at the interface completes the defect relations:

$$2C_\nu + C_{H+} = C_e. \quad (25)$$

Under conditions of the tests [6]:

$$p_{H_2O}(s) \approx p_{H_2O}(b) = 1\,\text{bar}. \quad (26)$$

Eqs. (21)–(26) can be solved and yield:

$$2\alpha C_{H+}^3 + C_{H+}^2 - \left(k\beta^{1/2}/\alpha\right)^{1/2} p_{H_2}(s)^{1/2} = 0. \quad (27)$$

In the tests performed under conditions of unlimited steam supply shown in Ref. [6], the surface ZrO_{2-x} composition is close to the stoichiometric one with substoichiometry deviation $x \le 10^{-5}$ [11]. In this case, Eq. (27) can be simplified, since C_ν being determined by x becomes extremely small $C_\nu/C_{Zr} \sim x \le 10^{-5}$ in comparison with the concentration of protons $C_{H+}/C_{Zr} \simeq 10^{-2}$–$10^{-3}$ (see below Eq. (31)):

$$C_{H+} \approx C_e. \quad (25')$$

Correspondingly, Eq. (27) can be also simplified:

$$C_{H+} = A\left(p_{H_2}(s)/RT\right)^{1/4} = A\left(c_1(s)\right)^{1/4}, \quad (27')$$

where $A = [k\beta^{1/2}/(\alpha RT)]^{1/4}$.

It should be noted that only in the case $C_{H+} \ll C_\nu$ (occurred, for example, under steam starvation conditions), the (usually proposed in the literature) neutrality condition $2C_\nu = C_e$ for the Zr oxidation in steam is valid. Therefore, the relation based on this last neutrality condition between the oxygen partial gas pressure p_{O_2} and the solid oxide substoichiometry deviation x which is used as a boundary condition in the problem of Zr oxidation in steam [11], turns to be inaccurate under the conditions of unlimited steam supply.

Under steam starvation conditions when $p_{H_2O}/p_{H_2} \to 0$ (instead of Eq. (26)) and $2C_\nu = C_e$ (instead of Eq. (25′)), for the proton concentration in oxide one gets

$$C_{H+} \propto p_{H_2O}^{1/3}\, p_{H_2}^{1/6}. \quad (28)$$

Therefore, under conditions of the tests [7] on the H_2 gas interactions with zirconia (i.e., $p_{H_2O} \to 0$) the proton concentration should turn to zero, $C_{H+} \to 0$, this is in accordance with observations [7] (since hydrogen was dissolved in zirconia in the form of neutral atoms rather than protons, see Section 2).

3.3. Mass transfer in the oxide phase

In the analysis of the tests [6] performed under conditions of unlimited steam supply it is naturally to assume that a relatively small amount of hydrogen dissolved in the oxide practically does not influence the stoichiometric composition of its surface. In the opposite case noticeable deviations of the oxidation kinetics from the parabolic time law should be expected. In reality such deviations were not observed in the tests [6] as well as in many other high temperature oxidation tests. Under such an assumption the oxygen flux in the oxide phase can be presented in the standard form:

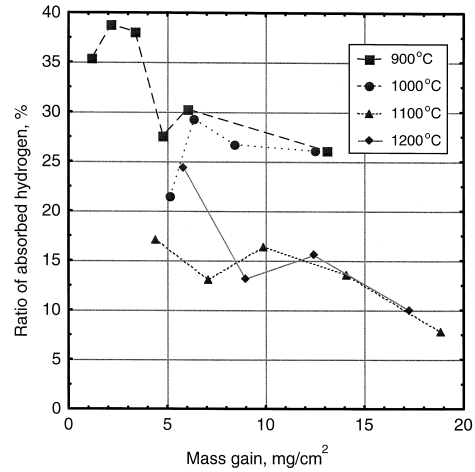

Fig. 3. Ratio of absorbed hydrogen in Zr–1Nb vs. mass gain during steam oxidation (from Ref. [6]).

$$J_O^{(ox)} = D_O^{(ox)}\Delta C_O/\delta(t), \quad (29)$$

where $D_O^{(ox)}$ is the oxygen diffusivity in the oxide, ΔC_O is the oxygen concentration fall across the oxide layer (invariable in time in accordance with the above mentioned assumption), $\delta(t) \propto t^{1/2}$ is the oxide layer thickness determined by the self-consistent solution of the oxygen diffusion problem in the multilayered system (gas/oxide/metal) and directly measured in the tests [6].

Analogous, the hydrogen flux in the oxide layer depends on the proton concentration fall $\Delta C_{H+} = C_{H+}(s) - C_{H+}(b)$ across this layer (see Fig. 8):

$$J_H^{(ox)} = D_H^{(ox)}\Delta C_{H+}/\delta(t), \quad (30)$$

where $D_H^{(ox)}$ is the hydrogen ion (protons) diffusivity in the oxide (estimated in [9] at 900 and 1000°C as 8×10^{-7} and 1.3×10^{-6} cm^2 s^{-1}, respectively; see Section 2); $C_{H+}(s)$ denotes hereafter the proton concentration at the gas/oxide interface (denoted above as C_{H+}). As noticed in [7] the value of $D_H^{(ox)}$ has the same order of magnitude as $D_O^{(ox)}$. Since the fluxes $J_O^{(ox)}$ and $J_H^{(ox)}$ have also comparable values within one order of magnitude (as follows from the measurements of absorbed to generated hydrogen ratio which varied in the tests [6] from 50 to 10%, see Fig. 3), the value ΔC_{H+} can be estimated as

$$\Delta C_{H+} \approx (0.1 - 1)\,\Delta C_O.$$

In the initial stage of the oxidation tests when $C_{H+}(s) \gg C_{H+}(b)$, this allows an estimation:

$$C_{H+}(s) \approx 10^{-4}\text{–}10^{-5}\ \mathrm{mol/cm^3},$$

or

$$C_{H+}/C_{Zr} \approx 10^{-2} - 10^{-3}. \quad (31)$$

It should be noted that in Eqs. (29) and (30) the quasistationary approximation for the diffusion problem in the oxide (well checked for oxygen and consequently for hydrogen, since $D_H^{(ox)} \approx D_O^{(ox)}$) was applied and for this reason linear concentration profiles in the oxide were taken.

3.4. Qualitative analysis of the model

In the initial stage of the oxidation process (when $C_{H+}(s) \gg C_{H+}(b)$ and the relative reduction of the metal layer thickness is small) a self-consistent solution of the problem of hydrogen mass transfer in the gas and oxide phases and absorption in the metal phase can be derived from the system of Eqs. (20), (27′), (29) and (30). The time dependence of hydrogen uptake can be analysed qualitatively from these equations.

Indeed, in this case $J_O^{(ox)} \sim J_H^{(ox)}$ as indicated in the previous section. Therefore, hydrogen concentration $c_1(s)$ in the gas near the interface can be estimated from Eq. (20):

$$c_1(s) \sim J_O^{(ox)}/k_1 \propto \delta(t)^{-1}$$

In accordance with Eq. (27′):

$$C_{H+}(s) \propto c_1(s)^{1/4} \propto \delta(t)^{-1/4}, \quad (32)$$

thus, substituting this last relationship into Eq. (30) one gets:

$$J_H^{(ox)} = D_H^{(ox)} \Delta C_{H+}/\delta(t) \propto \delta(t)^{-5/4} \propto t^{-5/8}.$$

Since this flux determines an amount of absorbed hydrogen in the metal phase $C_H(m)$:

$$\partial C_H^{(m)}/\partial t \propto J_H^{(ox)} \propto t^{-5/8},$$

finally one can get for the measured in [6] value:

$$C_H^{(m)} \propto t^{3/8}. \quad (33)$$

The accuracy of the hydrogen uptake measurements [6] is relatively low owing to small absolute values of the measured concentrations (10^2–10^3 ppm). Within these accuracy limits the difference between the obtained time dependencies $t^{3/8}$ and $t^{1/2}$ is insignificant, therefore, results of the measurements [6] at $t < 1000$ s (see Fig. 4) can be satisfactorily described by both the time laws. For this reason, a combination of the model constants determining coefficient B in the derived dependence $C_H^{(m)} = Bt^{3/8}$ can be obtained from the approximate linear dependence $C_H^{(m)}$ on $\Delta m \propto \delta(t) \propto t^{1/2}$ (in the initial stage of the process) measured in Ref. [6] and presented in Fig. 5.

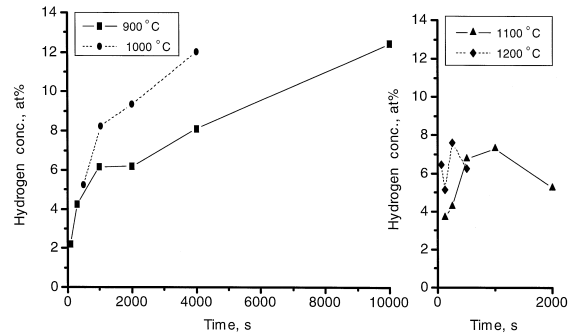

Fig. 4. Hydrogen concentration of Zr–1Nb samples after isothermal steam exposure (from Ref. [6]).

It is assumed that the hydrogen transition from the oxide to the metal phase as a result of the anodic reaction, Eq. (7):

$$H_{ab}^{+}(ox) + e_{\alpha}(ox/m) = H_{ab}(m)$$

is a quick process (in comparison with the bulk diffusion processes), so that the condition of thermodynamic equilibrium at the interface is valid. In this case the hydrogen concentration $C_{H+}(b)$ in the oxide near the oxide/metal interface increases along with $C_H^{(m)}$, these values being proportional to each other (see Eq. (34) below).

Simultaneously the hydrogen concentration $C_{H+}(s)$ in the oxide at the opposite interface decreases along with $c_1(s)$ in accordance with Eq. (32). Therefore, at some moment $t*$, the hydrogen concentration gradient across the oxide layer disappears (see Fig. 6a) and the flux $J_H^{(ox)}$ turns to zero (in accordance with Eq. (30)). Since $C_{H+}(s)$

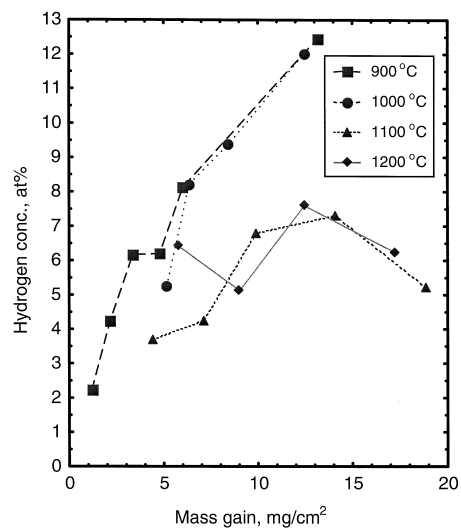

Fig. 5. Zr–1Nb hydrogen uptake vs. mass gain during steam oxidation (from Ref. [6]).

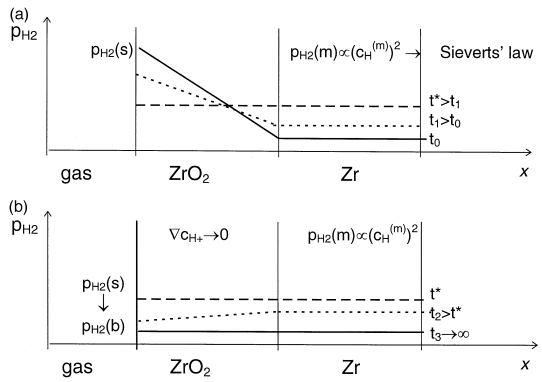

Fig. 6. (a) Schematic representation of hydrogen partial pressure distribution in the cladding layers in the initial stage of oxidation process. (b) Schematic representation of hydrogen partial pressure distribution in the cladding layers in the late stage of oxidation process.

continues to decrease, after this moment both ΔC_{H+} and $J_H^{(ox)}$ become negative and hydrogen desorption commences, leading to $C_H^{(m)}$ decrease.

Such a behaviour was observed in the tests [6] at 1100 and 1200°C (see Fig. 5). At lower temperatures 900 and 1000°C the tests were terminated before the moment of the absorption/desorption regime transformation. It is quite natural that at lower temperatures the period of absorption increases, since the hydrogen solubility in the metal phase also increases (in accordance with the equilibrium binary H/Zr phase diagram, Fig. 7).

At temperatures below 550°C the solubility of hydrogen atoms in the metal matrix drastically falls down (Fig. 7). For this reason the hydrogen concentration gradient in the oxide keeps a non-zero value for an extremely long period of time, and hydrogen transported by diffusion through the oxide along this gradient is continuously absorbed (after relatively quick saturation of the metal matrix) in the form of hydride precipitates.

After the above mentioned moment of the absorption/desorption regime transformation, the hydrogen flux in the oxide phase changes its direction and slightly increases from zero value providing desorption of hydrogen from the metal phase. However, it remains to be rather small since the diminishing of the partial hydrogen pressure $p_{H_2}(s) \propto c_1(s)$ at the oxide surface is a very slow process (along with the oxide layer growth) in a late stage of Zr oxidation. For this reason, the hydrogen concentration distribution in the oxide can be approximately considered as homogeneous: $C_{H+}(x) \approx C_{H+}(s)$ (see Fig. 6b). Thus, neglecting the hydrogen flux $J_H^{(ox)}$ in comparison with the oxygen flux $J_O^{(ox)}$, that results in $c_1(s) \approx J_O^{(ox)}/k_2$, and one can get a relationship analogous to Eq. (32): $C_{H+} \propto c_1(s)^{1/4} \propto \delta(t)^{-1/4}$, but for the spatially homogeneous concentration profile $C_{H+}(x) \approx C_{H+}$. As mentioned above, the boundary condition at the oxide/metal interface imposes a linear relation between this value C_{H+} and hydrogen concentration in the metal phase $C_H^{(m)}$ (see Eq. (34) below), which finally results in a slow reduction of the latter with time:

$$C_H^{(m)} \propto C_{H+} \propto \delta(t)^{-1/4} \propto t^{-1/8}.$$

This qualitative consideration of the hydrogen behaviour in the initial and late stages of the oxidation process is fairly well reproduced by more exact numerical calculations presented below in Section 4.

3.5. Mass transfer through the oxide / metal interface

For the quantitative description of the hydrogen uptake during all the oxidation period additional equations determining the hydrogen behaviour in the metal phase and at the oxide/metal interface should be derived. In accordance with the assumption about thermodynamic equilib-

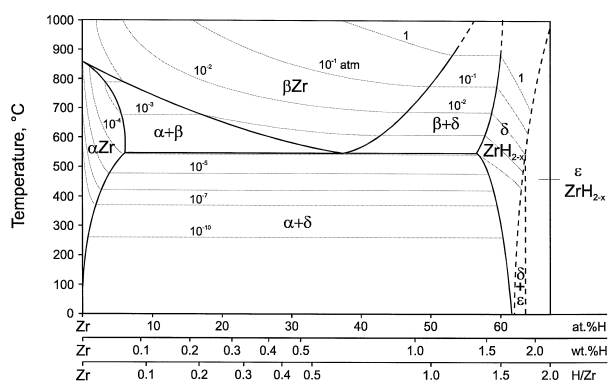

Fig. 7. Binary zirconium–hydrogen phase diagram and equilibrium hydrogen pressures (from Ref. [15]).

rium at the oxide/metal interface (see Section 3.4), both the anodic reactions described by Eqs. (4) and (7):

$$ZrO_2(ox) + 2V_o^{2+} + 4e_\alpha(m/ox) = Zr(m) + 2O_o(ox),$$

and

$$H_{ab}^{+}(ox) + e_\alpha(ox/m) = H_{ab}(m),$$

should be considered as equilibrium. Correspondingly, application of the mass action law for these reactions, taking into account that anion vacancy concentration is strictly determined by the limiting oxide non-stoichiometry in the binary Zr/O equilibrium phase diagram, results in a simple linear relation between interface hydrogen concentrations in the oxide $C_{H+}(b)$ and in the metal $C_H^{(m)}|_I$ (see Fig. 8):

$$C_{H+}(b) = \gamma C_H^{(m)}|_I \tag{34}$$

Therefore, Eq. (34) determines a boundary condition for the hydrogen diffusion problem in the metal phase which may be considered as a quasi-one-dimensional problem due to a small thickness of the cladding wall in comparison with its radius:

$$\partial C_H^{(m)}(x,t)/\partial t = D_H^{(m)}\partial^2 C_H^{(m)}(x,t)/\partial x^2,$$

where $D_H^{(m)}$ is the hydrogen diffusivity in the metal phase. Taking into account that $D_H^{(m)}$ is larger than the diffusivity in the oxide $D_H^{(ox)}$ by several orders of magnitude [12], with a sufficiently good accuracy one can consider the hydrogen distribution in the metal as homogeneous:

$$C_H^{(m)}(x,t) \approx C_H^{(m)}(t)|_1 \tag{35}$$

In this case the solution of the diffusion problem in the metal phase is reduced to the hydrogen balance equation (under one-side oxidation conditions):

$$d\left(L_m(t)C_H^{(m)}\right)/dt = J_H^{(ox)} - d\left[\delta(t)\left(C_{H+}(s) + C_{H+}(b)\right)/2\right]/dt, \tag{36}$$

where $L_m(t) = L_m(0) - \delta(t)/B$, is the metal layer thickness, $B \approx 1.5$ is the Pilling–Bedworth ratio, $J_H^{(ox)}$ is determined by Eq. (30).

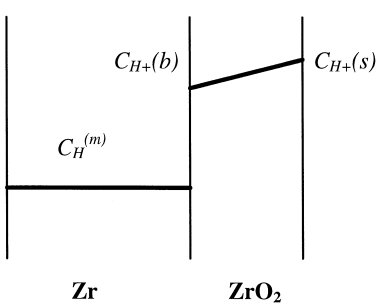

Fig. 8. Schematic representation of hydrogen concentration profiles in the oxide and metal phases.

Substituting Eqs. (30), (34) and (35) into Eq. (36) and neglecting a slow time variation of C_{H+} in comparison with that of $\delta(t)$ (see Eq. (32)) one can finally get

$$D_H^{(ox)}\left[\left(C_{H+}(s) - C_{H+}(b)\right)/\delta(t)\right] - 0.5\left(C_{H+}(s) + C_{H+}(b)\right)d\delta(t)/dt = d\left(L_m(t)C_H^{(m)}\right)/dt. \tag{37}$$

The self-consistent solution of Eq. (37) (appropriately modified for the case of double-side oxidation) together with Eqs. (20), (27′), (29) and (30) allows the calculation of the complicated dependence $C_H^{(m)}(t)$ measured in the tests [6].

4. Numerical solution of the model

A complete system of the Eqs. (20), (27), (29), (30), (34) and (37) describing the hydriding of the Zr cladding in the course of its oxidation in the steam atmosphere (after modification to the case of double-side oxidation) can be easily reduced to the following two equations:

$$dC_H^{(m)}/dt = \left(2D_H^{(ox)}/L_m(t)\right)\left(C_{H+}(S) - \gamma C_H^{(m)}\right)/\delta(t) - \left(C_H^{(m)}/L_m(t)\right)dL_m/dt - \left(1/L_m(t)\right)d \times \left[\delta\left(C_{H+}(S) + \gamma C_H^{(m)}\right)\right]/dt, \tag{38}$$

$$k_1\left(C_{H+}(S)/A\right)^4 + \left(D_H^{ox}/2\right)\left(C_{H+}(S) - \gamma C_H^{(m)}\right)/\delta(t) = D_O^{(ox)}\Delta C_O/\delta(t). \tag{39}$$

The parameters A and γ entering in the final Eqs. (38) and (39) are functions of the poorly known equilibrium constants of the interface chemical reactions, and currently the lacking experimental data cannot be calculated independently. However, these parameters may be explicitly derived within the framework of the present model by fitting of calculations to the experimental data [6]. Indeed, from Eqs. (38) and (39) it follows that the maximum value of the hydrogen concentration in the metal is roughly estimated as

$$C_H^{(m)}(\max) = (A/\gamma)\left(D_O^{(ox)}\Delta C_O/\delta(t)k_2\right)^{1/4}. \tag{40}$$

This maximum value is attained at time:

$$\tau_o = \left(L_m\alpha/D_H^{(ox)}\gamma\right)^2, \tag{41}$$

were α is the rate constant of the oxide scale growth: $\delta(t) = \alpha\sqrt{t}$. Hence, the knowledge of the maximum value of the hydrogen content in the metal and the hydriding kinetics allow the calculation of the two unknown thermodynamic parameters A and γ.

In the experiment [6], the hydrogen uptake was studied along with measurements of the Zr–1Nb cladding oxidation kinetics in the temperature range from 900 to 1200°C. By processing of the available data on mass gain and the ZrO_2 layer thickness growth kinetics (see, for example, Ref. [14]), the oxygen diffusion coefficient in the oxide

scale can be determined at different temperatures and approximated by the formula

$$D_{\mathrm{O}}^{(\mathrm{ox})} = 33.3\,\mathrm{e}^{-42\,418/RT}, \tag{42}$$

where T is in K, $R = 1.987$ cal/(mol K).

Wagner's data on the diffusivity of hydrogen ions in zirconia [9] refer to the yttria-stabilized samples. In the case of Zr–1Nb oxide these coefficients may be somewhat different. Lacking such data, however, the diffusion coefficients measured in Ref. [9] at 900 and 1000°C and extrapolated to the high temperature region,

$$D_{\mathrm{H}}^{(\mathrm{ox})} = 4\times10^{-4}\mathrm{e}^{-14\,405/RT}, \tag{43}$$

are used in the present calculations.

The other model parameters specifying conditions of the tests [6] are: $L_{\mathrm{m}}(0) = 0.07$ cm, $\delta(t) = 0.46\exp(-19\,919/RT)\sqrt{t}$ cm, ([6]), $\Delta C_0 = 7\times10^{-4}$ mol cm^{-3} (see, for example, Ref. [11]) and $k_2 = 75$ cm s^{-1}, in accordance with Eq. (10). As seen either from Eq. (40) or directly from Eq. (39), some underestimation of k_2 (discussed in Section 3.1) does not strongly influence the calculated value of A owing to a rather weak dependence of A on k_2.

In Fig. 9a and b experimental data [6] are compared with calculation results by the present model. The parameters A and γ obtained by fitting of experimental and theoretical data are shown in Table 1 and can be approximated by the formulas

$$A = 1.86–3.18(T/1000) + 1.38(T/1000)^2,$$

$$\left(\mathrm{mol/cm^3}\right)^{3/4}, \tag{44}$$

$$\gamma = 6.56–10.97(T/1000) + 4.63(T/1000)^2. \tag{45}$$

The values of γ obtained for 1100 and 1200°C seem to be too large, however, this can be attributed to an error of the hydrogen diffusion coefficient extrapolation by Eq. (43) to these temperatures (not measured directly). It can be shown that an enlargement of the diffusion coefficient value will result in proportional reduction of the calculated value of γ (see Eq. (41)).

In general, the calculations show that the hydrogen absorption by Zr–1Nb cladding during steam oxidation can be fairly well (practically within the accuracy of the experiment) represented by the model in the temperature range of the measurements [6] (from 900 to 1200°C).

Table 1
Calculated values of the model parameters A and γ

T,°C	A, (mol cm^{-3})$^{3/4}$	γ
900	0.032	0.005
1000	0.042	0.01
1100	0.11	0.18
1200	0.17	0.37

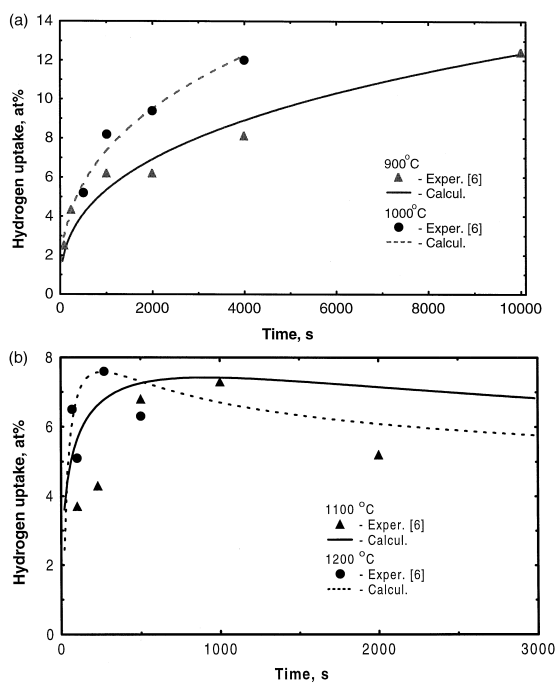

Fig. 9. (a) Comparison of the calculated and measured [6] hydrogen uptake by Zr–1Nb cladding during isothermal steam oxidation at $T = 900$ and 1000°C. (b) Comparison of the calculated and measured [6] hydrogen uptake by Zr–1Nb cladding during isothermal steam oxidation at $T = 1100$ and 1200°C.

5. Conclusions

In the present report, a model is developed for the description of hydrogen absorption by Zr alloys during oxidation in steam. The model is essentially based on the detailed experimental results of the recent tests [6] on the kinetics of hydrogen absorption by Zr–1Nb cladding during steam oxidation in the temperature range from 900 to 1200°C. Lacking exhaustive kinetic data at lower temperatures, the model was not attempted to be applied to the low temperature case, however, in general it corresponds qualitatively to numerous observations of significant hydrogen uptake (up to tens percents of a total amount of generated hydrogen) during Zr oxidation in a broader temperature range.

The main obstacle for an appropriate interpretation of this important phenomenon in the literature was connected with numerous results on gaseous hydriding of zirconia which directly evidenced that the hydrogen solubility and mobility in oxide layers are negligibly small. On this basis it was generally believed that a very thin oxide layer (with a thickness of several μm) on the metal surface protects

the metal substrate from hydrogen penetration, and the observed high values of hydrogen absorption during oxidation in steam were mainly associated with a defect structure (e.g., cracks or pores) of the growing protective oxide layer.

However, in surveying the results on hydrogen absorption one should distinguish between two possible routes; first, direct reaction with molecular hydrogen (gaseous hydriding), and second, absorption of hydrogen liberated by the decomposition of water or steam during the oxidation process and absorbed as part of the oxidation mechanism [1]. This conclusion can be indirectly confirmed by the results of Wagner's tests [9] on water vapour absorption by yttria-stabilized zirconia in which the dissolution process was interpreted in terms of the reaction, Eq. (1): $H_2O(g) + V_o^{2+} = 2H_i^+ + O_o(ox)$, with positively charged protons H^+ in the solid solution rather than neutral atoms characteristic for gaseous hydriding experiments (e.g., Ref. [7]). It was proposed in Ref. [7] that this fundamental difference in the two dissolution processes can explain an essential increase of the positively charged proton solubility and mobility (detected in Ref. [9]) in comparison with neutral H atoms.

On the basis of this important qualitative conclusion, the standard consideration of the steam oxidation process is modified in the framework of the coupled anodic/cathodic reactions at the two oxide interfaces (gas/oxide and oxide/metal) taking into account that hydrogen may intrude into the oxide in the result of a H_2O dissolution process governed by the same mechanism, Eq. (1) as observed in the tests [9], i.e., in the form of positively charged protons. Discharge of protons by electrons in this scheme occurs at the oxide/metal interface (rather than at the gas/oxide interface as considered in the standard approach) after diffusion transporting of highly mobile protons through the oxide scale.

For a quantitative description of the hydrogen behaviour by this mechanism, mass transfer in the three layers gas, oxide and metal, and at corresponding interfaces gas/oxide and oxide/metal, is considered.

For an appropriate description of the mass transfer through the gas phase, the standard approach for modelling of the multicomponent transport through the diffusion boundary layer in the gas mixture is modified and completed by consideration of (i) additional convective fluxes occurred owing to the absence of (usually assumed) equimolar counterdiffusion balance of H_2 and H_2O molecules, under conditions of hydrogen absorption and (ii) mutual transformation of the gas components owing to the equilibrium dissociation of H_2O molecules, $H_2O(g) = H_2(g) + (1/2)O_2(g)$, in the gas mixture.

Modelling of mass transfer through the oxide/gas interface is based on consideration of equilibrium kinetic processes in the vicinity of the oxide surface: (i) dissolution of water molecules in the oxide; (ii) dissociation of water molecules in the gas; (iii) oxygen transition from the oxide lattice sites to the gas phase; and (iv) hydrogen exchange between the solid and gas phases which are described by the corresponding mass action laws. In particular, such a consideration allows: (i) specification of the thermodynamic boundary conditions for oxygen and hydrogen species at the gas/oxide interface, inaccurately interpreted in the literature for the conditions of unlimited steam supply; and (ii) description consistent with observations [7] of hydrogen dissolution under steam starved conditions.

Mass transfer in the oxide phase is treated by self-consistent considerations of diffusion transport of oxygen ions and protons, with proton diffusion coefficients evaluated in Ref. [9] (at 900 and 1000°C).

Equilibrium conditions for oxygen and hydrogen species at the metal/oxide interface provide boundary conditions for the diffusion problem either in the oxide phase or in the metal phase. Owing to rather high hydrogen diffusivities in Zr (in comparison with that in the oxide phase), the latter problem can be reduced with a sufficient accuracy to a simple mass balance equation.

The obtained system of equations is qualitatively analysed explaining the main features of the observed complicated kinetics of hydrogen uptake: (i) continuous increase of hydrogen concentration in the metal phase being roughly proportional to the oxidation mass gain, in the initial stage of the process; (ii) desorption of hydrogen to the gas phase accompanied by a slow decrease of the measured hydrogen concentration in the metal phase, in the late stage of the process; (iii) decrease of the maximum hydrogen concentration in Zr attained at the absorption/desorption regime transformation, with temperature increase.

The numerical solution of the problem generally confirms the main conclusions of the simplified analytical treatment and furnishes a satisfactory fitting between measured kinetic curves [6] and calculations.

Acknowledgements

We are thankful to Drs P. Hofmann, V. Noack, G. Schanz, M. Steinbrück (FZK, Karlsruhe) and Dr. A. Palagin (IBRAE, Moscow) for valuable discussions and remarks. We are also grateful to Drs L. Maroti and L. Matus (KFKI, Hungary) for kind delivery of their paper [6] and valuable discussions, and to Professor D.R. Olander (University of California, Berkeley) for kind delivery of his paper [7].

Appendix A

In this Appendix, a derivation is presented of the H_2 and O_2 fluxes in the diffusion layer of the steam taking into account the dissociation/association of the H_2O

molecules in the gas mixture: $H_2O(g) = H_2(g) + (1/2)O_2(g)$. In accordance with this chemical reaction, there is a source for H_2 and O_2 molecules (and a corresponding sink for H_2O molecules) in each spatial point x of the gas phase. Mass transfer equations in the diffusion layer for the two components accordingly take form:

$$\partial c_1/\partial t = D_H \partial^2 c_1/\partial x^2 + Q(x,t), \quad (A.1)$$

$$\partial c_2/\partial t = D_O \partial^2 c_2/\partial x^2 + (1/2)Q(x,T), \quad (A.2)$$

where a value of the spatially distributed source $Q(x)$ is determined by the relation

$$Q(x) = k_1\left[c_3^2(x) - kc_1^2(x)c_2(x)\right], \quad (A.3)$$

the equilibrium constant $k = \exp(2\Delta G/RT)$ is determined by Eq. (16′), the kinetic constant k_1 specifies the velocity of the H_2O dissociation reaction, c_i is the molar density of the i-th component in the mixture, $i = 1,2,3$ denote H_2, O_2, H_2O, respectively (see Eq. (11)). Possible convection fluxes of the two components H_2 and O_2 are neglected in Eqs. (A.1) and (A.2) in accordance with estimations presented in Section 3. (see derivation of Eq. (20)).

Mass transfer in the gas phase is a very quick process in comparison with that in the solid oxide ($D_H \sim D_O \approx 10$ cm^2 s^{-1} at $T \approx 1000$°C), for this reason for the self-consistent solution of the Zr oxidation problem the quasistationary approximation for the gas phase is valid:

$$\partial c_1/\partial t \approx 0,\ \partial c_2/\partial t \approx 0. \quad (A.4)$$

Substituting Eqs. (A.3) and (A.4) into Eqs. (A.1) and (A.2) and integrating, one gets

$$D_H \partial c_1/\partial x + R(x,t) = A = \text{const.}, \quad (A.5)$$

$$D_O \partial c_2/\partial x + (1/2)R(x,t) = B = \text{const.}, \quad (A.6)$$

where

$$R(x) = \int Q(x)\,\mathrm{d}x.$$

Superposition of Eqs. (A.5) and (A.6) yields

$$\partial c_2/\partial x = (D_H/2D_O)\partial c_1/\partial x + M, \quad (A.7)$$

where

$$M = (2B - A)/2D_O = \text{const.}$$

Integration of Eq. (A.7) yields

$$c_2 = (D_H/2D_O)c_1 + Mx + N, \quad (A.8)$$

where $N = \text{const}$. By substitution of Eq. (A.8) into initial Eq. (A.1) taking into account Eqs. (A.3) and (A.4) one gets

$$D_H \partial^2 c_1/\partial x^2 + k_1\left[c_3^2 - kc_1^2\left((D_H/2D_O)c_1 + Mx + N\right)\right] = 0, \quad (A.9)$$

Local equilibration of the H_2O dissociation reaction is a much more quick process than the diffusion in the gas layer, that means

$$k_1 \gg D_H/L^2, \quad (A.10)$$

where L is the thickness of the diffusion boundary layer.

Indeed, at $T \approx 1000$°C, $k_1 \approx 10^6$–10^8 s^{-1} [13], whereas $D_H/L^2 \approx 10^2$ s^{-1} when $L \approx 0.3$ cm. Hence, under this approximation the diffusion term in Eq. (A.9) can be neglected, leading to

$$k_1\left[c_3^2 - kc_1^2\left((D_H/2D_O)c_1 + Mx + N\right)\right] \approx 0, \quad (A.11)$$

or, after transformation of the molar concentrations to the specific values: $C_i = c_i/c_g$, $i = 1,2,3$, with account of $C_3 \approx 1$ (since $c_1,\ c_2 \ll c_3$), finally, one gets

$$kc_g C_1^2\left[(D_H/2D_O)C_1 + mx + n\right] \approx 1, \quad (A.12)$$

where $m = M/c_g$, $n = N/c_g$, c_g is the molar concentration of the gas phase, $c_g = c_1 + c_2 + c_3$.

In order to determine the constants m and n, the obtained Eq. (A.12) should be substituted into boundary conditions at the oxide/gas interface:

$$x = 0,\ C_1 = C_1(\mathrm{s}),$$

and at the outer boundary of the diffusion layer:

$$x = L,\ C_1 = C_1(\mathrm{b}).$$

Differentiating Eq. (A.12):

$$\partial C_1/\partial x = -mC_1/\left(2mx + 1.5(D_H/D_O)C_1 + 2n\right),$$

and substituting the determined constants m and n, finally one gets

$$\partial c_1/\partial x|_{x=0} = -c_1(\mathrm{s})/L, \quad (A.13)$$

$$\partial c_2/\partial x|_{x=0} = -\left((D_H/D_O) - 1\right)c_2(\mathrm{b})/L, \quad (A.14)$$

(for comparison, the value of one of the derivatives at the opposite boundary can be also presented: $-\partial c_1/\partial x|_{x=L} = c_1(\mathrm{b})/L \ll -\partial c_1/\partial x|_{x=0}$).

It should be noted that to deduce the final Eqs. (A.13) and (A.14) the following inequalities were used: $c_2(\mathrm{s}) \gg c_2(\mathrm{b})$, $c_1(\mathrm{b}) \gg c_1(\mathrm{s})$, which were discussed in Section 3 (see derivation of Eq. (18)), and also $kc_1^2(\mathrm{b})c_1(\mathrm{s})/c_3 \gg 1$, which results from the relations $kc_1^2(\mathrm{b})c_2(\mathrm{b})/c_3 \simeq kc_1^3(\mathrm{b})/c_3 \simeq 1$ and $c_2(\mathrm{s}) \gg c_2(\mathrm{b})$.

References

[1] B. Cox, Adv. Corrosion Sci. Technol. 5 (1976) 173.
[2] J. Boehmert, M. Dietrich, J. Linek, Nucl. Energy Design 174 (1993) 53.
[3] J. Boehmert, J. Linek, M. Dietrich, Untersuchungen zur Hochtemperatur–Dampfoxidation von Zr 1% Nb, Zentralinstitut fuer Kernforschung Rossendorf bei Dresden, Report No. ZfK-743, 1991, p. 1.
[4] V. Vrtilkova, L. Molin, K. Kloc, V. Gamouz, Voprosy Atomnoi Nauki I Tehniki 27 (1988) 89, (in Russian).
[5] V.I. Dyachkov, Zh. Prikladnoi Chimii 64 (1991) 2029, (in Russian).
[6] J. Freska, G. Konczos, L. Maroti, L. Matus, Oxidation and hydriding of Zr 1% Nb alloys by steam, Report KFKI-1995-17/G, 1995.
[7] K. Park, D.R. Olander, J. Am. Ceram. Soc. 74 (1991) 72.
[8] K.-N. Choo, S.-I. Pyun, Y.-S. Kim, J. Nucl. Mater. 226 (1995) 9.
[9] C. Wagner, Ber. Bunsenges. Phys. Chem. 72 (1968) 778.
[10] V.G. Levich, Physico-Chemical Hydrodynamics, Moscow, 1959 (in Russian).
[11] D.R. Olander, Nucl. Eng. Design 148 (1994) 253.
[12] C. Katlinski, Inorg. Mater. 14 (1978) 1305.
[13] E.S. Shchetinnikov, Physics of Gas Combustion, Moscow, 1970 (in Russian).
[14] A.V. Berdyshev, L.V. Matveev, M.S. Veshchunov, Development of the data base for the kinetic model of the Zircaloy-4/steam oxidation at high temperatures ($1000°C \leq T \leq 1825°C$), Preprint IBRAE-97-05, Moscow, 1997.
[15] O. Kubaschewski-von Goldbeck, Physico-Chemical Properties of the Compounds and Alloys: Part II. Phase Diagrams, IAEA Special Issue, 6 (1976) 88–90.